

## Original Article

\*These authors contributed equally to this work.

**Cite this article:** Xue K, Liang S, Yang B, Zhu D, Xie Y, Qin W, Liu F, Zhang Y, Yu C (2022). Local dynamic spontaneous brain activity changes in first-episode, treatment-naïve patients with major depressive disorder and their associated gene expression profiles. *Psychological Medicine* **52**, 2052–2061. <https://doi.org/10.1017/S0033291720003876>

Received: 27 March 2020

Revised: 7 September 2020

Accepted: 28 September 2020

First published online: 30 October 2020

**Key words:**

Dynamic regional homogeneity; gene expression; imaging genetics; major depressive disorder; weighted gene co-expression network analysis

**Author for correspondence:** Feng Liu, E-mail: [fengliu@tjmu.edu.cn](mailto:fengliu@tjmu.edu.cn); Yong Zhang, E-mail: [zhangyong@tjmhc.com](mailto:zhangyong@tjmhc.com); Chunshui Yu, E-mail: [chunshuiyu@tjmu.edu.cn](mailto:chunshuiyu@tjmu.edu.cn)

# Local dynamic spontaneous brain activity changes in first-episode, treatment-naïve patients with major depressive disorder and their associated gene expression profiles

Kaizhong Xue<sup>1,\*</sup> , Sixiang Liang<sup>2,3,\*</sup>, Bingbing Yang<sup>1</sup>, Dan Zhu<sup>1</sup>, Yingying Xie<sup>1</sup>, Wen Qin<sup>1</sup>, Feng Liu<sup>1</sup>, Yong Zhang<sup>2</sup> and Chunshui Yu<sup>1,4</sup>

<sup>1</sup>Department of Radiology and Tianjin Key Laboratory of Functional Imaging, Tianjin Medical University General Hospital, Tianjin 300052, China; <sup>2</sup>Tianjin Anding Hospital, Tianjin 300222, China; <sup>3</sup>The National Clinical Research Center for Mental Disorders & Beijing Key Laboratory of Mental Disorders, Beijing Anding Hospital, Capital Medical University & the Advanced Innovation Center for Human Brain Protection, Capital Medical University, Beijing 100088, China and <sup>4</sup>CAS Center for Excellence in Brain Science and Intelligence Technology, Chinese Academy of Sciences, Shanghai 200031, China

**Abstract**

**Background.** Major depressive disorder (MDD) is a common debilitating disorder characterized by impaired spontaneous brain activity, yet little is known about its alterations in dynamic properties and the molecular mechanisms associated with these changes.

**Methods.** Based on the resting-state functional MRI data of 65 first-episode, treatment-naïve patients with MDD and 66 healthy controls, we compared dynamic regional homogeneity (dReHo) of spontaneous brain activity between the two groups, and we investigated gene expression profiles associated with dReHo alterations in MDD by leveraging transcriptional data from the Allen Human Brain Atlas and weighted gene co-expression network analysis.

**Results.** Compared with healthy controls, patients with MDD consistently showed reduced dReHo in both fusiform gyri and in the right temporal pole and hippocampus. The expression profiles of 16 gene modules were correlated with dReHo alterations in MDD. These gene modules were enriched for various biological process terms, including immune, synaptic signalling, ion channels, mitochondrial function and protein metabolism, and were preferentially expressed in different cell types.

**Conclusions.** Patients with MDD have reduced dReHo in brain areas associated with emotional and cognitive regulation, and these changes may be related to complex polygenic and polypathway mechanisms.

**Introduction**

Major depressive disorder (MDD) is a leading cause of disability worldwide, affecting 350 million people each year (World Health Organization, 2008). The conditions of more than half of patients with MDD become chronic or recurrent after the first depressive episode, resulting in huge economic and medical burdens (Cuijpers, Beekman, & Reynolds, 2012). Although substantial efforts have been made in the past decade, the pathophysiological mechanism of MDD remains largely unknown.

Resting-state functional magnetic resonance imaging (rs-fMRI) is increasingly emerging as a promising tool to delineate spontaneous brain activity of the human brain, which has prominent advantages in clinical research due to the minimal need for cooperation from patients. Previous studies have demonstrated altered resting-state spontaneous brain activity in MDD via various approaches (Fitzgerald, Laird, Maller, & Daskalakis, 2008; Geng et al., 2019; Guo et al., 2011a, 2011b; Xia et al., 2019), among which regional homogeneity (ReHo) shows high reproducibility (Zang, Jiang, Lu, He, & Tian, 2004) and has been repeatedly reported to be changed in MDD (Lai, 2018; Sun et al., 2018; Xia et al., 2019). However, ReHo can reflect only static temporal synchronization of spontaneous brain activity among nearby voxels, which is inconsistent with the concept that spontaneous brain activity is a time-dependent dynamic process (Hutchison et al., 2013). In recent years, dynamic functional connectivity has been used to assess large-scale dynamic patterns of temporal synchronization of spontaneous brain activity between spatially remote brain regions/voxels (Friston, 2011; Hutchison et al., 2013), and its changes have been reported in neuropsychiatric diseases, including schizophrenia (Sakoglu et al., 2010), Alzheimer's disease (de Vos et al., 2018), epilepsy (Liu et al., 2017), and MDD (Demirtaş et al., 2016; Han et al., 2019; Kaiser et al., 2016; Qiu et al., 2018). However, few studies have focused on the dynamic properties of regional temporal synchronization of spontaneous brain activity among nearby voxels, which can be

measured by dynamic ReHo (dReHo). Furthermore, no studies have investigated dReHo changes in MDD.

MDD has an estimated heritability of approximately 37% (Sullivan, Neale, & Kendler, 2000); however, reproducible risk loci of MDD rarely have been identified in previous genome-wide association studies (GWASs) (Howard et al., 2018, 2019, Sullivan et al., 2009; Wray et al., 2018), possibly due to the inadequate sample size. As intermediate phenotypes, neuroimaging features of MDD are theoretically closer to genetic substrates of MDD (Gottesman & Gould, 2003). In addition, gene expression is theoretically closer to neuroimaging features of MDD than genetic variants. Therefore, several studies have used cross-sample or cross-region spatial correlation analysis to investigate associations between brain gene expression and neuroimaging features of major psychiatric disorders and have achieved great success (Liu, Tian, Li, Li, & Zhuo, 2019; Morgan et al., 2019; Romero-Garcia, Warriner, Bullmore, Baron-Cohen, & Bethlehem, 2019; Romme, de Reus, Ophoff, Kahn, & van den Heuvel, 2017). Nevertheless, no transcription-neuroimaging association studies have been carried out to identify genes whose brain expression profiles are correlated with dReHo changes in MDD.

We hypothesize that brain gene expression is related to regional spontaneous brain activity changes in MDD. Here, gene expression data were derived from six postmortem brains provided by the Allen Human Brain Atlas (AHBA) (Hawrylycz et al., 2015), and regional spontaneous brain activity was assessed by dReHo since it is more consistent with the fact that brain activity is dynamic (Hutchison et al., 2013). We then identified genes associated with dReHo changes in MDD by performing cross-sample spatial correlations between gene expression data from the postmortem AHBA brains and case-control dReHo differences from living human brains. Finally, the function of the identified genes associated with dReHo changes in MDD was explored by several enrichment analyses. An overview of the analytical framework is summarized in Fig. 1.

## Materials and methods

### Subjects

Sixty-seven first-episode, treatment-naïve patients with MDD were recruited from Tianjin Medical University General Hospital. MDD was diagnosed based on the diagnostic criteria of the Structure Clinical Interview of DSM-IV (SCID). Following previous studies (Khan, Bhat, Kolts, Thase, & Brown, 2010), we recruited only MDD patients with Hamilton Depression Rating Scale-17 (HDRS-17) scores  $\geq 18$ . The Hamilton Anxiety Rating Scale-14 (HARS-14) was used to evaluate anxiety symptoms in these patients, but we did not set a cut-off value. Moreover, patients with other psychiatric diseases, including schizophrenia, bipolar disorder, mental retardation and personality disorder, were excluded. A total of 69 age- and sex-matched healthy controls were recruited from the local community, and the SCID Non-Patient Edition was used to confirm that they were free of any psychiatric disorders. Common exclusion criteria for all participants were (1) age younger than 18 years or older than 65 years; (2) left-handedness; (3) the presence of organic intracranial lesions; (4) any history of comorbid alcohol or drug abuse; (5) poor image quality; and (6) MRI contradictions. The Ethics Institution of Tianjin Medical University General Hospital approved the study protocol and written informed consent was obtained from participants.

### Image acquisition

All MRI images were obtained using a 3.0-Tesla Discovery MR750 scanner (General Electric, Milwaukee, WI). Foam paddings and ear-plugs were utilized to minimize head movement and reduce noise. The rs-fMRI data were obtained using a single-shot gradient-recalled-echo echo-planar-imaging (SS-GRE-EPI) sequence with the following parameters: repetition time (TR) = 2000 ms; echo time (TE) = 30 ms; field of view (FOV) = 220 mm  $\times$  220 mm; matrix = 64  $\times$  64; flip angle (FA) = 90°; slice thickness = 3 mm, no gap; 36 interleaved transverse slices; and 180 volumes. During the fMRI scanning, subjects were asked to close their eyes, hold still, think of nothing in particular, and not fall asleep. Sagittal 3D T1-weighted images were acquired by a brain volume sequence using the following parameters: TR = 8.14 ms; TE = 3.17 ms; inversion time = 450 ms; FOV = 256 mm  $\times$  256 mm; matrix = 256  $\times$  256; FA = 12°; slice thickness = 1 mm, no gap; and 188 slices.

### Image preprocessing

The imaging quality of each subject was carefully examined, and subjects with poor imaging quality were excluded. The rs-fMRI data were preprocessed using the Data Processing Assistant for Resting-State fMRI (DPARSF) (Chao-Gan & Yu-Feng, 2010) based on Statistical Parametric Mapping 12 (<http://www.fil.ion.ucl.ac.uk/spm>). Briefly, the first ten volumes were discarded to allow the signal to reach equilibrium and the remaining 170 volumes were corrected for temporal differences between slices and head motion. Participants with maximum displacement  $>2.0$  mm and maximum rotation  $>2.0^\circ$  were excluded from the subsequent analyses. In addition, the mean framewise displacement (FD) (Van Dijk, Sabuncu, & Buckner, 2012) was calculated. Subsequently, individual structural images were co-registered to the mean functional image, and then the transformed structural images were segmented into grey matter, white matter and cerebrospinal fluid. Based on these segmented images, the normalization parameters from individual native space to Montreal Neurological Institute (MNI) space were estimated by the Diffeomorphic Anatomical Registration Through Exponentiated Lie algebra (DARTEL) tool (Ashburner, 2007). The motion-corrected functional imaging data were normalized to MNI space using these normalization parameters and resampled to 3-mm cubic voxels. Spurious variances were removed by regression, including linear drift, Friston-24 head motion parameters (Friston, Williams, Howard, Frackowiak, & Turner, 1996), and signals from white matter and cerebrospinal fluid. Finally, temporal bandpass filtering (0.01–0.08 Hz) was applied to reduce the effects of low-frequency drift and high-frequency noise.

### dReHo calculation

dReHo was calculated using the sliding window approach with the Data Processing & Analysis of Brain Imaging (DPABI) toolbox (Yan, Wang, Zuo, & Zang, 2016). Since there is no consensus on the selection of window length and step size, we calculated individual dReHo maps (Fig. 1a and online Supplementary Table S1) based on 25 combinations of the two parameters (window lengths: 18, 34, 50, 66, 82 TRs; step sizes: 1, 2, 3, 4, 5 TRs) that have been used in prior studies (Hutchison & Morton, 2015; Leonardi & Van De Ville, 2015; Li, Duan, Cui, Chen, & Liao, 2019; Li, Lu, & Yan, 2020; Liao et al., 2014). For each combination, ReHo was computed for each sliding window and then

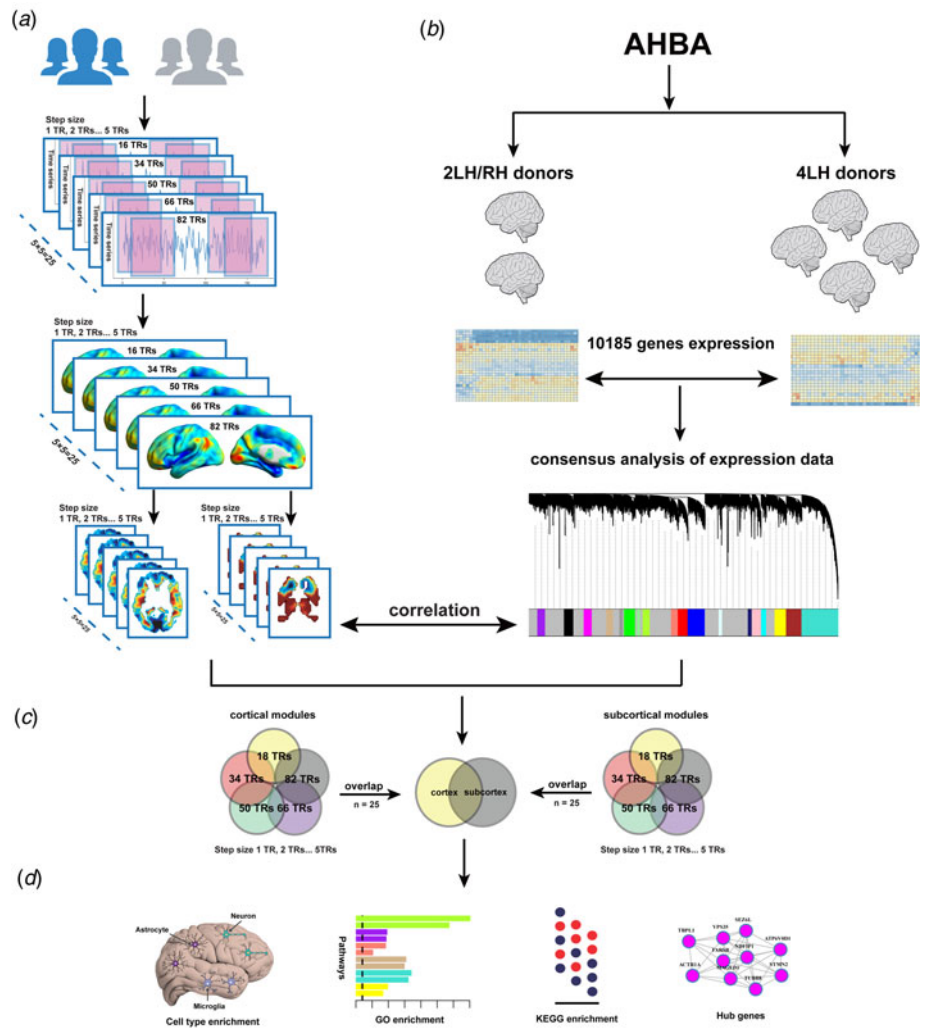


**Fig. 1.** Overview of the analysis pipeline. (a) a sliding window method was utilized to compute dReHo, and between-group comparisons of dReHo maps were performed; (b) the association between dReHo differences and gene expression from the AHBA was explored; (c) stable cortical and subcortical modules related to MDD were identified; (d) enrichment analysis was applied for these modules. dReHo, dynamic regional homogeneity; AHBA, Allen Human Brain Atlas.

the standard deviation was calculated across these ReHo maps to characterize the dReHo. The dReHo maps were finally smoothed with a Gaussian kernel of 8-mm full width at half-maximum.

### dReHo comparison

Voxel-wise two-sample  $t$  tests were performed to identify dReHo differences between the two groups in each combination (five window lengths and five step sizes), and 25  $t$ -maps were generated while adjusting for age, sex and mean FD. Multiple comparisons were corrected by the topological false discovery rate (FDR) method (the initial height threshold: uncorrected  $p < 0.001$ ; topological FDR:  $q < 0.05$ ). The topological FDR is an extension of the Benjamini-Hochberg FDR (BH-FDR) and is specially designed to correct multiple comparisons in neuroimaging analyses (Chumbley, Worsley, Flandin, & Friston, 2010). To reduce the influence of the selection of window lengths and step sizes on the dReHo differences between groups, we created a probability map to show highly consistent brain regions with significant differences in dReHo calculated by different parametric combinations. In addition, mean dReHo values of clusters with 100% probability were extracted to perform partial correlations between dReHo and clinical variables (HDRS, HARS and illness duration) in patients with MDD while adjusting for age, sex, and mean FD. Given that whole-brain coverage including the cerebellum and

brain stem was not available for all subjects, we restricted between-group comparisons to within the cerebrum.

### Gene expression data preprocessing

Publicly available gene expression data of six postmortem neurotypical adult brains were obtained from the AHBA database (Hawrylycz *et al.*, 2012), which, in total, consists of normalized microarray expression data of more than 20 000 genes measured in 3702 brain samples. Among them, four donors had expression data only in the left hemisphere, and two donors had expression data in both hemispheres. Based on the newly proposed pipeline (Arnatkevic Iūtė, Fulcher, & Fornito, 2019), we separately processed the two datasets and obtained two sample  $\times$  gene expression matrices of  $1196 \times 10\,185$  from the four donors and  $1209 \times 10\,185$  from the two donors (Fig. 1b and online Supplementary Material). Here, the samples represent brain tissue samples, and the screening process of tissue samples is provided in online Supplementary Fig. S1.

### Creation of gene modules

Weighted gene co-expression network analysis (WGCNA) is an effective tool that clusters genes into network modules and detects biologically meaningful results (Zhang & Horvath, 2005).

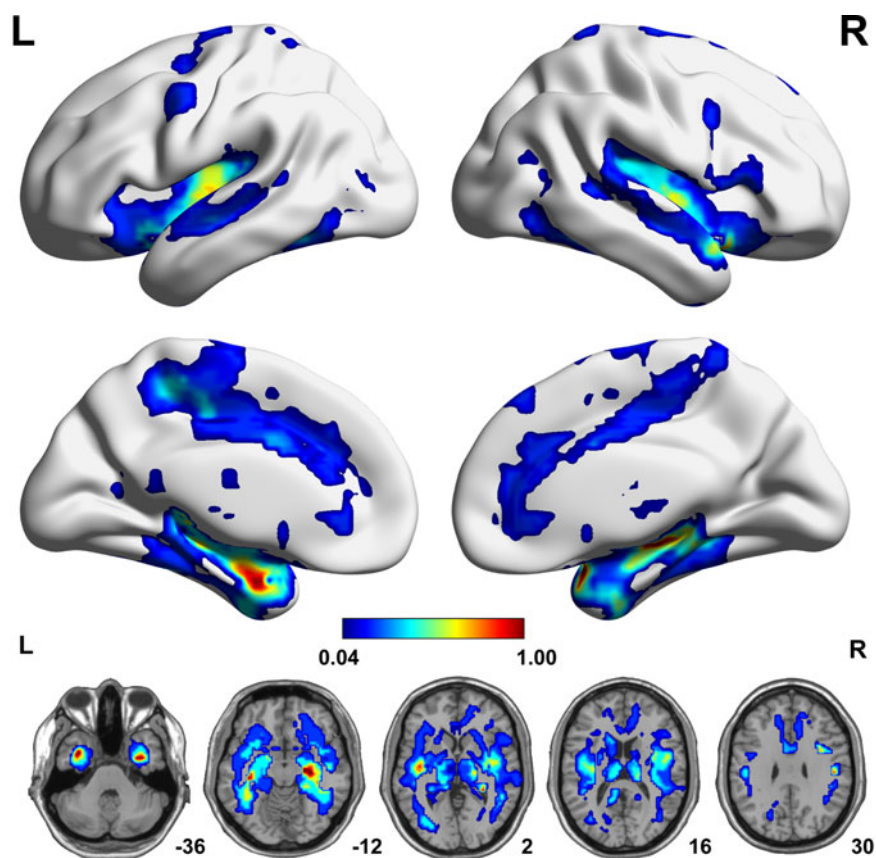


**Fig. 2.** A probability map showing brain voxels with significant dReHo differences ( $q < 0.05$ , topological FDR corrected) between the MDD and HC groups. The colour bar represents the probability of a given voxel showing a significant intergroup difference in the 25 comparisons. Each comparison is performed on individual dReHo maps calculated by a distinct combination of dynamic parameters. FDR, false discovery rate; HC, healthy control; L, left; MDD, major depressive disorder; R, right.

Therefore, we first constructed a signed network for each sample  $\times$  gene expression matrix. Then, a WGCNA consensus network was created from two networks to identify common expression patterns across the two aforementioned expression matrices, and 19 gene modules were finally obtained (online Supplementary material, Supplementary Fig. S2 and Table S2). For each module, the expression pattern (a matrix represented by sample  $\times$  number of genes in this module) was summarized by the first principal component, defined as the module eigengene (ME, number of samples  $\times$  1 vector).

#### Transcription-neuroimaging association analysis

To establish the sample correspondence between gene expression and neuroimaging data, we defined a 6-mm radius sphere centred at the MNI coordinate of each tissue sample and extracted the mean value on each  $t$ -statistical map of dReHo difference (25  $t$ -statistical maps). Then, for each module, we calculated Pearson's correlation between the ME and the  $t$ -value across brain tissue samples. The correlation analysis was performed separately for the cortical and subcortical samples because of great differences in gene expression profiles between cortical and subcortical regions (Hawrylycz et al., 2012). Multiple comparisons were corrected using the BH-FDR method ( $q < 0.05$ ). Gene modules with significant correlations between the ME and the  $t$ -value in cortical samples were defined as cortical modules, and subcortical modules were defined by the same approach. As shown in Fig. 1c, based on the results of correlation analyses, we first intersected the results of 25 combinations of dynamic parameters in cortical and subcortical modules, respectively.

The cortical/subcortical modules that were correlated with all  $t$ -statistical maps derived from different combinations were considered stable modules. Then, the stable cortical and subcortical gene modules were also intersected to identify shared and distinct gene modules for cortical and subcortical regions.

#### Enrichment analysis

Enrichment analysis (Fig. 1d) for stable modules was mainly performed by the web server g:Profiler (<https://biit.cs.ut.ee/gprofiler>), including the Gene Ontology (GO) and Kyoto Encyclopedia of Genes and Genomes (KEGG) databases and putative transcription factor binding sites (TFBS) from the TRANSFAC database (Reimand et al., 2016). All the 10 185 included genes were defined as a background gene set, and the AutoAnnotate Cytoscape application (Shannon et al., 2003) was used to show the enrichment results. In addition, cell-type enrichment analysis was conducted using Fisher's exact test with a specificity index probability ( $pSI$ ) (Dougherty, Schmidt, Nakajima, & Heintz, 2010) of 0.05 (BH-FDR correction) based on previously published gene expression data for different cell types of the human brain (Zhang et al., 2016).

## Results

#### Demographic information and clinical characteristics

After excluding two subjects (one patient and one control) due to poor image quality and three subjects (one patient and two controls) due to excessive head motion, 65 MDD patients and 66 healthy controls were finally included in this study. The

demographic and clinical data of these subjects are displayed in online Supplementary Table S3. The two groups did not show significant differences in sex (chi-squared test,  $p = 0.78$ ), age (two-sample  $t$  test,  $p = 0.65$ ), or mean FD (two-sample  $t$  test,  $p = 0.31$ ).

### Case-control difference in dReHo

Based on individual dReHo maps from each of the 25 parametric combinations, we compared voxel-wise dReHo differences between patients with MDD and healthy controls ( $q < 0.05$ , topological FDR corrected), from which we created a probability map (Fig. 2) to show the probability of a given voxel with a significant intergroup difference in these comparisons. Compared with healthy controls, patients with MDD consistently (100% probability) showed significantly decreased dReHo in both fusiform gyri and the right hippocampus and temporal pole (superior part) (Fig. 2 and online Supplementary Table S4). We did not find significantly increased dReHo in any comparisons in patients with MDD relative to healthy controls. We also tested the impact of HARS score on our results, but we did not find significant effects (online Supplementary Results and Supplementary Fig. S3).

### Correlations between dReHo and clinical variables

The mean dReHo values of clusters with consistent (100% probability) reduction in patients with MDD were extracted. Partial correlation analysis was conducted between the mean dReHo values and clinical variables, including HARS and HDRS scores and illness duration, while adjusting for age, sex, and FD. No significant correlations (all  $p > 0.05$ ) were found between dReHo and any clinical variables in patients with MDD.

### Transcription-neuroimaging associations

Nineteen consensus modules were identified from WGCNA analysis based on expression data from four left-hemispheric and two bi-hemispheric brain samples (Fig. 3). Cross-sample Pearson's correlation was calculated between MEs of each module and dReHo differences to show the consistent correlation pattern of modules across the two expression datasets and the 25 combinations. The results showed that there were 16 consistently significant MDD-related modules, 14 of which belonged to cortical modules and six of which belonged to subcortical modules (overlapping four modules) (Figs. 4 and 5a). The positive correlation means that brain regions with significant dReHo reduction in MDD show higher gene expression, and the negative correlation means that those regions show lower gene expression (online Supplementary Figs. S4 and S5).

### Enrichment analysis

GO enrichment analysis was conducted for each preserved module (see detailed results in online Supplementary Data Table S1). Genes in these preserved modules were enriched for pathways related to synaptic signalling, adenosine triphosphate synthesis, epithelial regulation, immune response, the regulation of transcription and translation, protein localization and metabolic regulation, ion channel activities, mitochondrial function, axon ensheathment and central nervous system development. KEGG enrichment analysis revealed that genes in these preserved modules were related to the glutamatergic system, serotonergic system, neurodegenerative diseases (such as Alzheimer's disease,

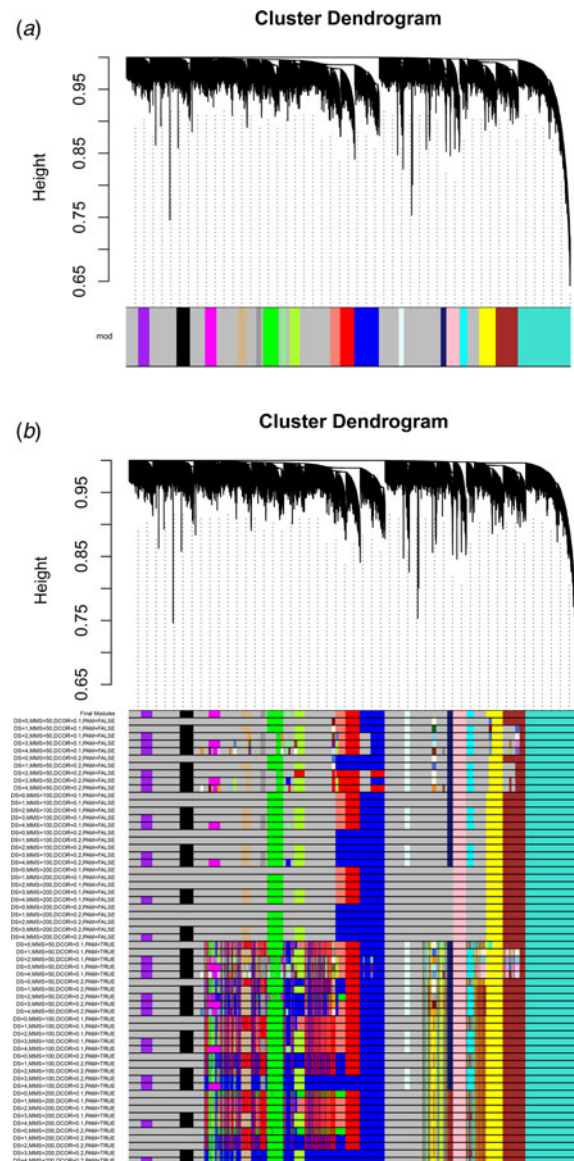


**Fig. 3.** Consensus analysis of expression data. (a) WGCNA dendrogram showing consensus modules based on the topological co-expression of 10 185 genes from four left hemispheres and two whole brains. (b) To avoid the scenario that co-expression networks constructed accidentally based on the set of WGCNA parameters used, we rebuilt networks by applying different parameter sets. The final consensus modules used in this study were conserved among the majority of the tests with different parameter sets. WGCNA, weighted gene co-expression network analysis.

Parkinson disease and Huntington disease), autoimmune diseases and circadian rhythms (Figs. 5b, c, online Supplementary Tables S5 and S6). As illustrated in Fig. 5d and online Supplementary Table S7, there were seven preserved modules specifically enriched for neurons, two for astrocytes, two for microglia, one for endothelial cells and one for oligodendrocytes. Moreover, TFBS enrichment showed that 11 out of 16 preserved modules were related to transcriptional control (online Supplementary Table S8 and Data Table S1).

### Discussion

To our knowledge, this is the first attempt to apply dReHo to investigate regional temporal synchronization changes in

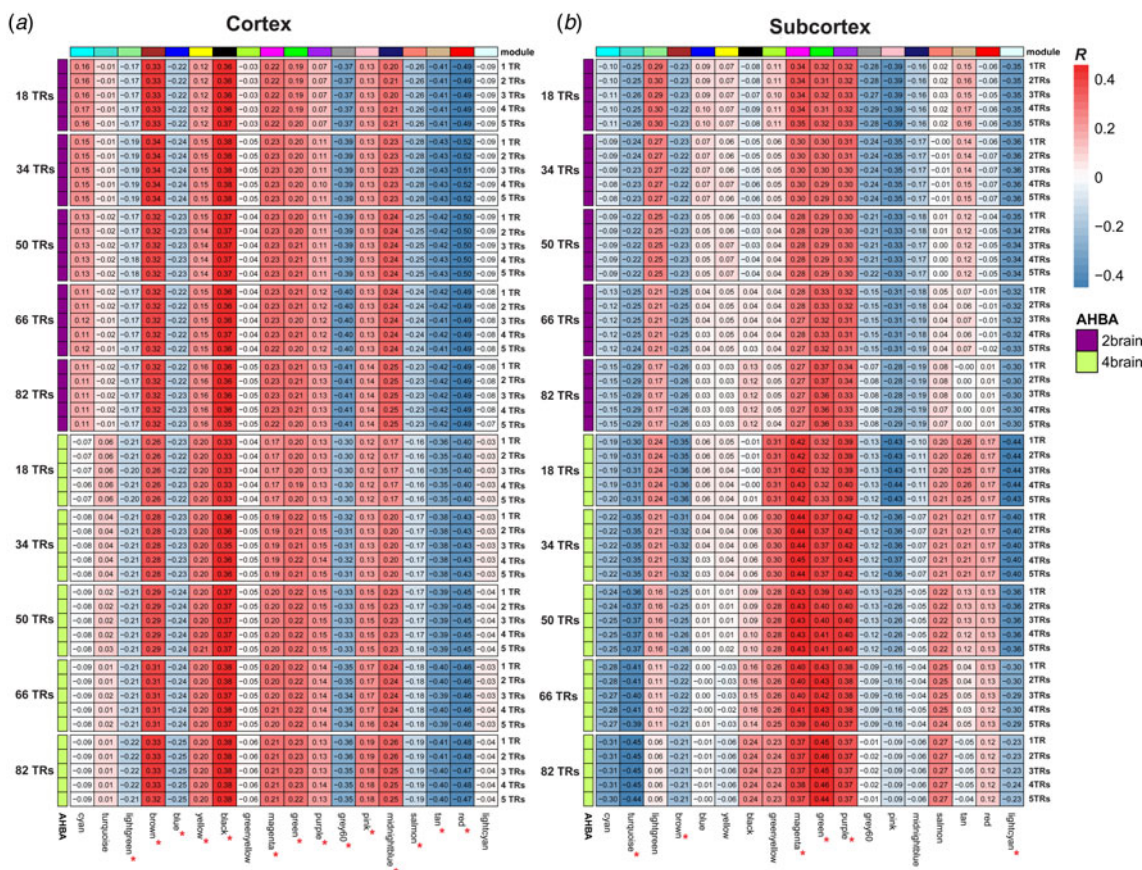


**Fig. 4.** Correlations between gene expression and dReHo changes in MDD. (a) The heatmap shows Pearson's correlation coefficients between MEs of gene modules and *t* values of case-control dReHo differences in cortical samples. Each column represents a gene module (*n* = 18), and each row represents a case-control dReHo difference map derived from dReHo maps calculated with a given combination (*n* = 25) of window size and step size. In the rows of the upper half, gene expression data were obtained from two AHBra donors with whole-brain coverage; in the rows of the lower half, however, they were obtained from four AHBra donors only with left-brain coverage. (b) The heatmap shows correlations in subcortical samples. \* indicates that the correlation reaches the significance of *q* < 0.05 (BH-FDR corrected) in all analyses. The colour bar represents Pearson's correlation coefficients between MEs of gene modules and *t* values of case-control dReHo differences.

spontaneous brain activity in first-episode, treatment-naïve patients with MDD and, in parallel, to directly correlate brain gene expression with case-control dReHo differences to explore gene modules associated with dReHo changes in MDD and to characterize the involved biological pathways.

In the present study, we observed that first-episode, treatment-naïve patients with MDD consistently showed significantly decreased dReHo in the fusiform gyrus, hippocampus and temporal pole, which were present in all 25 combinations of window lengths and step sizes. The fusiform gyrus is involved in the processing of emotional faces (Kanwisher, McDermott, & Chun, 1997; Weiner & Grill-Spector, 2010). Thus, our finding of reduced dReHo in the fusiform gyrus supports and extends previous reports of the structural and functional impairments in this area in MDD (Schmaal et al., 2017; Truong et al., 2013). As an association area, the temporal pole is involved in various high-level cognitive functions, such as facial recognition (Olsson & Ochsner, 2008), memory (Munoz-Lopez, Mohedano-Moriano, & Insausti, 2010), and language processing (Hickok & Poeppel, 2007). This structure also plays a role in emotion regulation and the theory of mind mainly by interacting with the amygdala and orbital frontal cortex (Frith & Frith, 2010), which also showed a high probability of having decreased dReHo in patients with MDD. Moreover, this result extends the finding of the reduced

static ReHo in MDD (Guo et al., 2011b; Liu et al., 2010) to the impairment of regional dynamics of temporal synchronization of spontaneous brain activity in the disorder. It has been widely accepted that exposure to life stress is a major risk factor for MDD (McEwen, 2008), which is related to the fact that overwhelming stress can impair normal hippocampal function. An increasing number of studies have demonstrated that the hippocampus is highly sensitive to stress (Pittenger & Duman, 2008), the most important environmental risk factor for the development of MDD (Kessler, 1997) and it is also the main target associated with the genetic risk of MDD (Xu et al., 2018). This is why our study and others always show hippocampal impairment in patients with MDD (Gold, 2015; Liu et al., 2013). Taking previous and our findings together, we propose that functional impairment in the cognition- and emotion-regulatory networks is an important feature of MDD.

Unexpectedly, we did not find any significant correlations between dReHo values in the consistently reduced dReHo regions and clinical variables (HARS and HDRS scores and illness duration) in patients with MDD. The reasons for the non-significant findings are elusive, but they may be related to the clinical features of patients (first-episode, treatment-naïve), the lack of clinical assessments (such as rumination) reflecting other aspects of MDD, the relatively short illness duration, and others. Thus, the

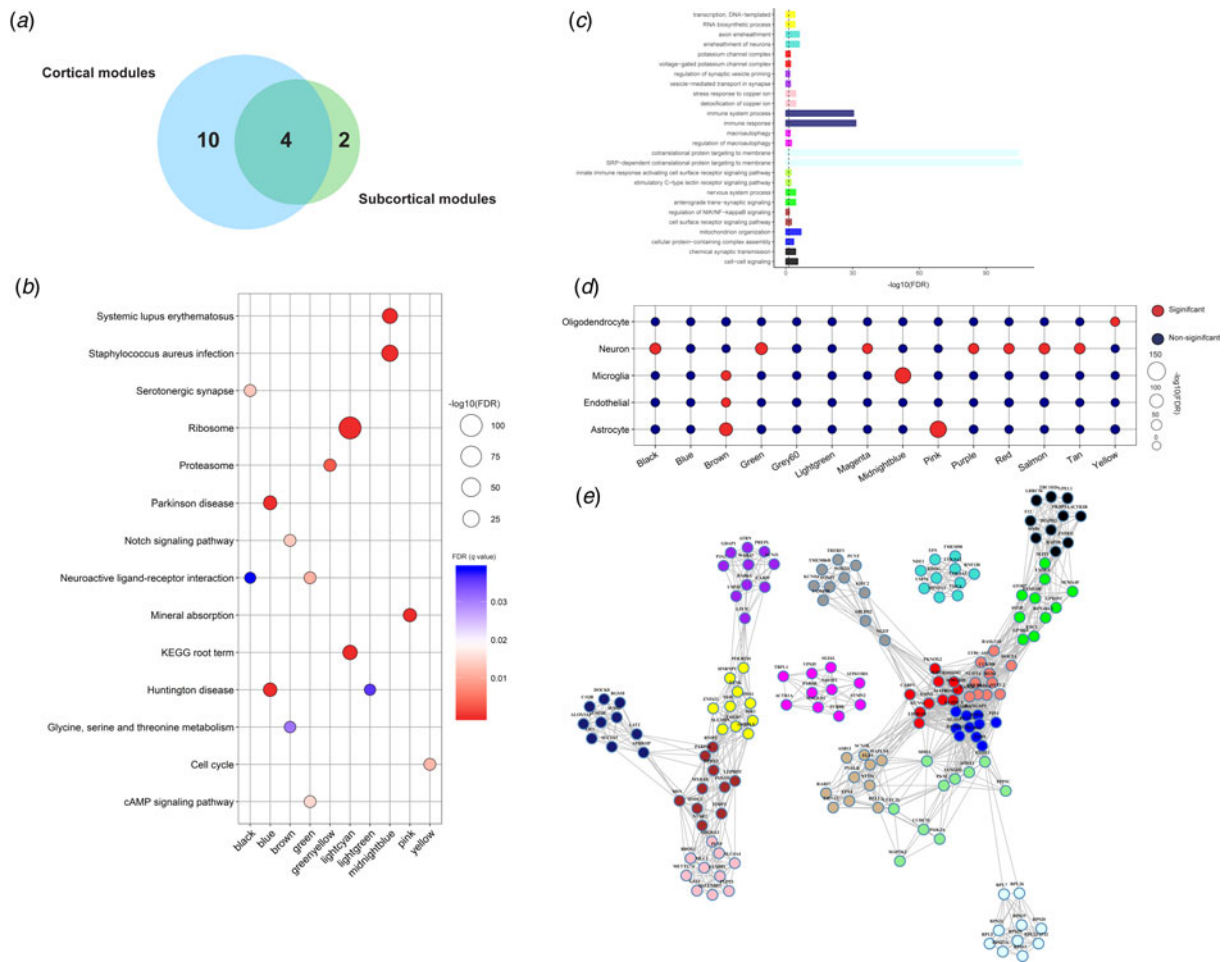


**Fig. 5.** Enrichment of genes in stable modules and hub genes. (a) Counts of MDD-related cortical and subcortical modules. (b) KEGG enrichment for genes in all modules (top two pathways shown for each module). All obtained results could pass  $q < 0.05$  (BH-FDR correction) and showed odds ratios  $> 1$ . (c) GO enrichment for genes in all modules (top two pathways shown for each module marked by different colour). The bubble size represents significance for  $-\log_{10}$ FDR (BH-FDR correction), and the bubble colour represents whether the module is significant or not. (d) The top 10 hub genes are shown for all MDD-related modules. Edges are weighted by the strength of correlation between nodes (genes). KEGG, Kyoto Encyclopedia of Genes and Genomes; GO, Gene Ontology.

clinical value of dReHo changes in MDD needs to be clarified in future studies.

In contrast to previous GWASs that failed to identify reproducible risk loci of MDD (Howard *et al.*, 2018, 2019; Sullivan *et al.*, 2009; Wray *et al.*, 2018), by combining an endophenotype (dReHo) of MDD and brain gene expression data, we found a dozen gene modules with various functions associated with dReHo changes in MDD, indicating that MDD may develop via complex polygenetic and polypathway mechanisms. Gene expression profiles in both cortical and subcortical areas, in multiple cell types, in different biological functions and pathways might be related to the development of MDD. Gene expression in both cortical and subcortical areas was associated with dReHo changes in MDD, mimicking the pattern of the brain structural and functional changes in this disorder (Chen *et al.*, 2012; Liu *et al.*, 2013; Ma *et al.*, 2012; Vasic, Walter, Hose, & Wolf, 2008). The co-existence of the shared and specific gene modules between cortical and subcortical areas reflects the complexity of the molecular substrates of MDD. This complexity was also supported by the involvement of the related gene modules in various cell types, biological functions and pathways. For example, several modules

enriched for neurons were mainly implicated in synaptic transmission and neuronal development, indicating that neuronal impairment and maldevelopment may be possible mechanisms of MDD (Krishnan & Nestler, 2008; Willner, Scheel-Kruger, & Belzung, 2013). Several modules enriched for microglia are mainly implicated in the immune system, which is consistent with the stress model of MDD via microglial activation and the inflammatory response (Felger & Lotrich, 2013; Hodes, Kana, Menard, Merad, & Russo, 2015; Setiawan *et al.*, 2015). Since dReHo is calculated based on blood-oxygen-level-dependent (BOLD) signals, the association of dReHo changes in MDD with the expression profiles of gene modules enriched for neurons, astrocytes and endothelial cells is consistent with the neurovascular coupling theory of BOLD signals because these cells are the main components of the neurovascular unit (Iadecola, 2017; Muoio, Persson, & Sendeski, 2014). These findings indicate that impaired neurovascular coupling may also contribute to depressive symptoms. In addition, the enrichment of MDD-related genes for neurodegenerative diseases may be a reflection of the shared assaulting target (such as hippocampus) by the risk factors for these disorders (Xu *et al.*, 2018). Moreover, hub gene detection

can provide candidate genes for further studies. For example, several immune-related genes were identified by hub gene detection, which may be used to explore the immune mechanism of MDD.

At least two limitations should be considered when interpreting our findings. The first limitation is that gene expression data and brain imaging data were not obtained from the same subjects. The identified correlations between gene expression data from six postmortem brains and brain imaging data from other living human brains may be correct only if gene expression profiles are highly conserved across individuals. That is, this study would inevitably miss genes or gene modules with great individual differences. Since gene expression profiles are dependent on age, sex, and ethnicity (Mogil et al., 2018; Somel et al., 2010), the mismatch of age, sex, and ethnicity between expression and imaging data may introduce bias to this study. Another limitation is the impact of the selection of dynamic parameters on the calculation of dReHo. Although we used 25 combinations of dynamic parameters to identify consistent results, the development of strategies to select the optimal combination of parameters is still critically important.

In this study, we found that first-episode, treatment-naïve patients with MDD showed reduced dReHo in the regulatory networks of cognition and emotion, indicating that functional abnormalities in these networks are important features of MDD. The case-control differences in dReHo showed replicable spatial correlations with the expression profiles of gene modules associated with various cell types, biological functions and pathways, indicating that MDD may develop via complex polygenetic and poly pathway mechanisms.

**Supplementary material.** The supplementary material for this article can be found at <https://doi.org/10.1017/S0033291720003876>.

**Acknowledgements.** We thank the Allen Institute for Brain Science founders and staff who supplied the brain expression data. This study was funded by the National Key Research and Development Program of China (2018YFC1314300), the National Natural Science Foundation of China (82030053 and 82072001), the Tianjin Key Technology R&D Program (17ZXMSFY00090), and the Natural Science Foundation of Tianjin Municipal Science and Technology Commission (18JCQNJC10900).

#### Author contributions.

Kaizhong Xue and Sixiang Liang made substantial contributions to the conception and design of the work and to the acquisition, analysis, and interpretation of data, and they drafted the manuscript. Bingbing Yang, Dan Zhu and Yingying Xie helped draft the manuscript. Wen Qin and Feng Liu critically revised the manuscript for important intellectual content. Yong Zhang and Chunshui Yu approved the final version of the manuscript to be published and agreed to be accountable for all aspects of the work, ensuring that questions related to the accuracy or integrity of any part of the work were appropriately investigated and resolved. All authors read, critically revised, and approved the manuscript.

**Conflict of interest.** None.

**Ethical standards.** The authors assert that all procedures contributing to this work comply with the ethical standards of the relevant national and institutional committees on human experimentation and with the Helsinki Declaration of 1975, as revised in 2008.

## References

- Arnatkeviciūtė, A., Fulcher, B. D., & Fornito, A. (2019). A practical guide to linking brain-wide gene expression and neuroimaging data. *Neuroimage*, 189, 353–367. doi: 10.1016/j.neuroimage.2019.01.011.
- Ashburner, J. (2007). A fast diffeomorphic image registration algorithm. *Neuroimage*, 38(1), 95–113. doi: 10.1016/j.neuroimage.2007.07.007.
- Chao-Gan, Y., & Yu-Feng, Z. (2010). DPARSF: A MATLAB toolbox for “pipeline” data analysis of resting-state fMRI. *Frontiers in Systems Neuroscience*, 4, 13. doi: 10.3389/fnsys.2010.00013.
- Chen, J. D., Liu, F., Xun, G. L., Chen, H. F., Hu, M. R., Guo, X. F., ... Zhao, J. P. (2012). Early and late onset, first-episode, treatment-naïve depression: Same clinical symptoms, different regional neural activities. *Journal of Affective Disorders*, 143(1–3), 56–63. doi: 10.1016/j.jad.2012.05.025.
- Chumbley, J., Worsley, K., Flandin, G., & Friston, K. (2010). Topological FDR for neuroimaging. *Neuroimage*, 49(4), 3057–3064. doi: 10.1016/j.neuroimage.2009.10.090.
- Cuijpers, P., Beekman, A. T. F., & Reynolds, C. F., 3rd. (2012). Preventing depression: A global priority. *JAMA*, 307(10), 1033–1034. doi: 10.1001/jama.2012.271.
- Demirtaş, M., Tornador, C., Falcón, C., López-Solà, M., Hernández-Ribas, R., Pujol, J., ... Deco, G. (2016). Dynamic functional connectivity reveals altered variability in functional connectivity among patients with major depressive disorder. *Human Brain Mapping*, 37(8), 2918–2930. doi: 10.1002/hbm.23215.
- de Vos, F., Koini, M., Schouten, T. M., Seiler, S., van der Grond, J., Lechner, A., ... Rombouts, S. (2018). A comprehensive analysis of resting state fMRI measures to classify individual patients with Alzheimer’s disease. *Neuroimage*, 167, 62–72. doi: 10.1016/j.neuroimage.2017.11.025.
- Dougherty, J. D., Schmidt, E. F., Nakajima, M., & Heintz, N. (2010). Analytical approaches to RNA profiling data for the identification of genes enriched in specific cells. *Nucleic Acids Research*, 38(13), 4218–4230. doi: 10.1093/nar/gkq130.
- Felger, J. C., & Lotrich, F. E. (2013). Inflammatory cytokines in depression: Neurobiological mechanisms and therapeutic implications. *Neuroscience*, 246, 199–229. doi: 10.1016/j.neuroscience.2013.04.060.
- Fitzgerald, P. B., Laird, A. R., Maller, J., & Daskalakis, Z. J. (2008). A meta-analytic study of changes in brain activation in depression. *Human Brain Mapping*, 29(6), 683–695. doi: 10.1002/hbm.20426.
- Friston, K. J. (2011). Functional and effective connectivity: A review. *Brain Connectivity*, 1(1), 13–36. doi: 10.1089/brain.2011.0008.
- Friston, K. J., Williams, S., Howard, R., Frackowiak, R. S., & Turner, R. (1996). Movement-related effects in fMRI time-series. *Magnetic Resonance in Medicine*, 35(3), 346–355. doi: 10.1002/mrm.1910350312.
- Frith, U., & Frith, C. (2010). The social brain: Allowing humans to boldly go where no other species has been. *Philosophical Transactions of the Royal Society of London. Series B, Biological Sciences*, 365(1537), 165–176. doi: 10.1098/rstb.2009.0160.
- Geng, J., Yan, R., Shi, J., Chen, Y., Mo, Z., Shao, J., ... Lu, Q. (2019). Altered regional homogeneity in patients with somatic depression: A resting-state fMRI study. *Journal of Affective Disorders*, 246, 498–505. doi: 10.1016/j.jad.2018.12.066.
- Gold, P. W. (2015). The organization of the stress system and its dysregulation in depressive illness. *Molecular Psychiatry*, 20(1), 32–47. doi: 10.1038/mp.2014.163.
- Gottesman, I. I., & Gould, T. D. (2003). The endophenotype concept in psychiatry: Etymology and strategic intentions. *The American Journal of Psychiatry*, 160(4), 636–645. <https://doi.org/10.1176/appi.ajp.160.4.636>.
- Guo, W. B., Liu, F., Xue, Z. M., Yu, Y., Ma, C. Q., Tan, C. L., ... Zhao, J. P. (2011a). Abnormal neural activities in first-episode, treatment-naïve, short-illness-duration, and treatment-response patients with major depressive disorder: A resting-state fMRI study. *Journal of Affective Disorders*, 135(1–3), 326–331. doi: 10.1016/j.jad.2011.06.048.
- Guo, W. B., Sun, X. L., Liu, L., Xu, Q., Wu, R. R., Liu, Z. N., ... Zhao, J. P. (2011b). Disrupted regional homogeneity in treatment-resistant depression: A resting-state fMRI study. *Progress in Neuro-Psychopharmacology & Biological Psychiatry*, 35(5), 1297–1302. doi: 10.1016/j.pnpbp.2011.02.006.
- Han, S., Wang, X., He, Z., Sheng, W., Zou, Q., Li, L., ... Chen, H. (2019). Decreased static and increased dynamic global signal topography in major depressive disorder. *Progress in Neuro-Psychopharmacology & Biological Psychiatry*, 94, 109665. doi: 10.1016/j.pnpbp.2019.109665.
- Hawrylycz, M. J., Lein, E. S., Guillozet-Bongaarts, A. L., Shen, E. H., Ng, L., Miller, J. A., ... Jones, A. R. (2012). An anatomically comprehensive atlas of the adult human brain transcriptome. *Nature*, 489(7416), 391–399. doi: 10.1038/nature11405.

- Hawrylycz, M., Miller, J. A., Menon, V., Feng, D., Dolbeare, T., Guillozet-Bongaarts, A. L., ... Lein, E. (2015). Canonical genetic signatures of the adult human brain. *Nature Neuroscience*, *18*(12), 1832–1844. doi: 10.1038/nn.4171.
- Hickok, G., & Poeppel, D. (2007). The cortical organization of speech processing. *Nature Reviews Neuroscience*, *8*(5), 393–402. doi: 10.1038/nrn2113.
- Hodes, G. E., Kana, V., Menard, C., Merad, M., & Russo, S. J. (2015). Neuroimmune mechanisms of depression. *Nature Neuroscience*, *18*(10), 1386–1393. doi: 10.1038/nn.4113.
- Howard, D. M., Adams, M. J., Clarke, T.-K., Hafferty, J. D., Gibson, J., Shirali, M., ... McIntosh, A. M. (2019). Genome-wide meta-analysis of depression identifies 102 independent variants and highlights the importance of the prefrontal brain regions. *Nature Neuroscience*, *22*(3), 343–352. doi: 10.1038/s41593-018-0326-7.
- Howard, D. M., Adams, M. J., Shirali, M., Clarke, T. K., Marioni, R. E., Davies, G., ... McIntosh, A. M. (2018). Genome-wide association study of depression phenotypes in UK biobank identifies variants in excitatory synaptic pathways. *Nature Communications*, *9*(1), 1470. doi: 10.1038/s41467-018-03819-3.
- Hutchison, R. M., & Morton, J. B. (2015). Tracking the brain's functional coupling dynamics over development. *The Journal of Neuroscience: The Official Journal of the Society for Neuroscience*, *35*(17), 6849–6859. doi: 10.1523/jneurosci.4638-14.2015.
- Hutchison, R. M., Womelsdorf, T., Allen, E. A., Bandettini, P. A., Calhoun, V. D., Corbetta, M., ... Chang, C. (2013). Dynamic functional connectivity: Promise, issues, and interpretations. *Neuroimage*, *80*, 360–378. doi: 10.1016/j.neuroimage.2013.05.079.
- Iadecola, C. (2017). The neurovascular unit coming of age: A journey through neurovascular coupling in health and disease. *Neuron*, *96*(1), 17–42. doi: 10.1016/j.neuron.2017.07.030.
- Kaiser, R. H., Whitfield-Gabrieli, S., Dillon, D. G., Goer, F., Beltzer, M., Minkel, J., ... Pizzagalli, D. A. (2016). Dynamic resting-state functional connectivity in major depression. *Neuropsychopharmacology*, *41*(7), 1822–1830. doi: 10.1038/npp.2015.352.
- Kanwisher, N., McDermott, J., & Chun, M. M. (1997). The fusiform face area: A module in human extrastriate cortex specialized for face perception. *The Journal of Neuroscience: The Official Journal of the Society for Neuroscience*, *17*(11), 4302–4311. doi: 10.1523/JNEUROSCI.17-11-04302.1997.
- Kessler, R. C. (1997). The effects of stressful life events on depression. *Annual Review of Psychology*, *48*, 191–214. doi: 10.1146/annurev.psych.48.1.191.
- Khan, A., Bhat, A., Kolts, R., Thase, M. E., & Brown, W. (2010). Why has the antidepressant-placebo difference in antidepressant clinical trials diminished over the past three decades? *CNS Neuroscience & Therapeutics*, *16*(4), 217–226. doi: 10.1111/j.1755-5949.2010.00151.x.
- Krishnan, V., & Nestler, E. J. (2008). The molecular neurobiology of depression. *Nature*, *455*(7215), 894–902. doi: 10.1038/nature07455.
- Lai, C.-H. (2018). The regional homogeneity of cingulate-precuneus regions: The putative biomarker for depression and anxiety. *Journal of Affective Disorders*, *229*, 171–176. doi: 10.1016/j.jad.2017.12.086.
- Leonardi, N., & Van De Ville, D. (2015). On spurious and real fluctuations of dynamic functional connectivity during rest. *Neuroimage*, *104*, 430–436. doi: 10.1016/j.neuroimage.2014.09.007.
- Li, J., Duan, X., Cui, Q., Chen, H., & Liao, W. (2019). More than just statics: Temporal dynamics of intrinsic brain activity predicts the suicidal ideation in depressed patients. *Psychological Medicine*, *49*(5), 852–860. doi: 10.1017/S0033291718001502.
- Li, L., Lu, B., & Yan, C. G. (2020). Stability of dynamic functional architecture differs between brain networks and states. *Neuroimage*, *216*, 116230. doi: 10.1016/j.neuroimage.2019.116230.
- Liao, W., Zhang, Z., Mantini, D., Xu, Q., Ji, G. J., Zhang, H., ... Lu, G. (2014). Dynamical intrinsic functional architecture of the brain during absence seizures. *Brain Structure & Function*, *219*(6), 2001–2015. doi: 10.1007/s00429-013-0619-2.
- Liu, F., Guo, W., Liu, L., Long, Z., Ma, C., Xue, Z., ... Chen, H. (2013). Abnormal amplitude low-frequency oscillations in medication-naïve, first-episode patients with major depressive disorder: A resting-state fMRI study. *Journal of Affective Disorders*, *146*(3), 401–406. doi: 10.1016/j.jad.2012.10.001.
- Liu, F., Tian, H., Li, J., Li, S., & Zhuo, C. (2019). Altered voxel-wise gray matter structural brain networks in schizophrenia: Association with brain genetic expression pattern. *Brain Imaging and Behavior*, *13*(2), 493–502. doi: 10.1007/s11682-018-9880-6.
- Liu, F., Wang, Y., Li, M., Wang, W., Li, R., Zhang, Z., ... Chen, H. (2017). Dynamic functional network connectivity in idiopathic generalized epilepsy with generalized tonic-clonic seizure. *Human Brain Mapping*, *38*(2), 957–973. doi: 10.1002/hbm.23430.
- Liu, Z., Xu, C., Xu, Y., Wang, Y., Zhao, B., Lv, Y., ... Du, C. (2010). Decreased regional homogeneity in insula and cerebellum: A resting-state fMRI study in patients with major depression and subjects at high risk for major depression. *Psychiatry Research*, *182*(3), 211–215. doi: 10.1016/j.psychres.2010.03.004.
- Ma, C., Ding, J., Li, J., Guo, W., Long, Z., Liu, F., ... Chen, H. (2012). Resting-state functional connectivity bias of middle temporal gyrus and caudate with altered gray matter volume in major depression. *PLoS ONE*, *7*(9), e45263. doi: 10.1371/journal.pone.0045263.
- McEwen, B. S. (2008). Understanding the potency of stressful early life experiences on brain and body function. *Metabolism: Clinical and Experimental*, *57*(Suppl 2), S11–15. doi: 10.1016/j.metabol.2008.07.006.
- Mogil, L. S., Andaleon, A., Badalamenti, A., Dickinson, S. P., Guo, X., Rotter, J. I., ... Wheeler, H. E. (2018). Genetic architecture of gene expression traits across diverse populations. *PLoS Genetics*, *14*(8), e1007586. doi: 10.1371/journal.pgen.1007586.
- Morgan, S. E., Seidlitz, J., Whitaker, K. J., Romero-Garcia, R., Clifton, N. E., Scarpazza, C., ... Bullmore, E. T. (2019). Cortical patterning of abnormal morphometric similarity in psychosis is associated with brain expression of schizophrenia-related genes. *Proceedings of the National Academy of Sciences of the United States of America*, *116*(19), 9604–9609. doi: 10.1073/pnas.1820754116.
- Munoz-Lopez, M. M., Mohedano-Moriano, A., & Insausti, R. (2010). Anatomical pathways for auditory memory in primates. *Frontiers in Neuroanatomy*, *4*, 129. doi: 10.3389/fnana.2010.00129.
- Muoio, V., Persson, P. B., & Sendeski, M. M. (2014). The neurovascular unit – concept review. *Acta Physiologica (Oxford, England)*, *210*(4), 790–798. doi: 10.1111/apha.12250.
- Olsson, A., & Ochsner, K. N. (2008). The role of social cognition in emotion. *Trends in Cognitive Sciences*, *12*(2), 65–71. doi: 10.1016/j.tics.2007.11.010.
- Pittenger, C., & Duman, R. S. (2008). Stress, depression, and neuroplasticity: A convergence of mechanisms. *Neuropsychopharmacology: Official Publication of the American College of Neuropsychopharmacology*, *33*(1), 88–109. doi: 10.1038/sj.npp.1301574.
- Qiu, L., Xia, M., Cheng, B., Yuan, L., Kuang, W., Bi, F., ... Gong, Q. (2018). Abnormal dynamic functional connectivity of amygdalar subregions in untreated patients with first-episode major depressive disorder. *Journal of Psychiatry & Neuroscience: JPN*, *43*(4), 262–272. doi: 10.1503/jpn.170112.
- Reimand, J., Arak, T., Adler, P., Kolberg, L., Reisberg, S., Peterson, H., & Vilo, J. (2016). g:Profiler – a web server for functional interpretation of gene lists (2016 update). *Nucleic Acids Research*, *44*(W1), W83–W89. doi: 10.1093/nar/gkwl199.
- Romero-Garcia, R., Warrier, V., Bullmore, E. T., Baron-Cohen, S., & Bethlehem, R. A. I. (2019). Synaptic and transcriptionally downregulated genes are associated with cortical thickness differences in autism. *Molecular Psychiatry*, *24*(7), 1053–1064. doi: 10.1038/s41380-018-0023-7.
- Romme, I. A., de Reus, M. A., Ophoff, R. A., Kahn, R. S., & van den Heuvel, M. P. (2017). Connectome disconnectivity and cortical gene expression in patients with schizophrenia. *Biological Psychiatry*, *81*(6), 495–502. doi: 10.1016/j.biopsych.2016.07.012.
- Sakoglu, U., Pearlson, G. D., Kiehl, K. A., Wang, Y. M., Michael, A. M., & Calhoun, V. D. (2010). A method for evaluating dynamic functional network connectivity and task-modulation: Application to schizophrenia. *Magma (New York, N.Y.)*, *23*(5–6), 351–366. doi: 10.1007/s10334-010-0197-8.
- Schmaal, L., Hibar, D. P., Samann, P. G., Hall, G. B., Baune, B. T., Jahanshad, N., ... Veltman, D. J. (2017). Cortical abnormalities in adults and adolescents with major depression based on brain scans from 20 cohorts worldwide in the ENIGMA Major Depressive Disorder Working Group. *Molecular Psychiatry*, *22*(6), 900–909. doi: 10.1038/mp.2016.60.

- Setiawan, E., Wilson, A. A., Mizrahi, R., Rusjan, P. M., Miler, L., Rajkowska, G., ... Meyer, J. H. (2015). Role of translocator protein density, a marker of neuroinflammation, in the brain during major depressive episodes. *JAMA Psychiatry*, *72*(3), 268–275. doi: 10.1001/jamapsychiatry.2014.2427.
- Shannon, P., Markiel, A., Ozier, O., Baliga, N. S., Wang, J. T., Ramage, D., ... Ideker, T. (2003). Cytoscape: A software environment for integrated models of biomolecular interaction networks. *Genome Research*, *13*(11), 2498–2504. doi: 10.1101/gr.1239303.
- Somel, M., Guo, S., Fu, N., Yan, Z., Hu, H. Y., Xu, Y., ... Khaitovich, P. (2010). MicroRNA, mRNA, and protein expression link development and aging in human and macaque brain. *Genome Research*, *20*(9), 1207–1218. doi: 10.1101/gr.106849.110.
- Sullivan, P. F., de Geus, E. J., Willemsen, G., James, M. R., Smit, J. H., Zandbelt, T., ... Penninx, B. W. (2009). Genome-wide association for major depressive disorder: A possible role for the presynaptic protein piccolo. *Molecular Psychiatry*, *14*(4), 359–375. doi: 10.1038/mp.2008.125.
- Sullivan, P. F., Neale, M. C., & Kendler, K. S. (2000). Genetic epidemiology of major depression: Review and meta-analysis. *The American Journal of Psychiatry*, *157*(10), 1552–1562. doi: 10.1176/appi.ajp.157.10.1552.
- Sun, H., Luo, L., Yuan, X., Zhang, L., He, Y., Yao, S., ... Xiao, J. (2018). Regional homogeneity and functional connectivity patterns in major depressive disorder, cognitive vulnerability to depression and healthy subjects. *Journal of Affective Disorders*, *235*, 229–235. doi: 10.1016/j.jad.2018.04.061.
- Truong, W., Minuzzi, L., Soares, C. N., Frey, B. N., Evans, A. C., MacQueen, G. M., & Hall, G. B. (2013). Changes in cortical thickness across the lifespan in major depressive disorder. *Psychiatry Research*, *214*(3), 204–211. doi: 10.1016/j.pscychresns.2013.09.003.
- Van Dijk, K. R., Sabuncu, M. R., & Buckner, R. L. (2012). The influence of head motion on intrinsic functional connectivity MRI. *Neuroimage*, *59*(1), 431–438. doi: 10.1016/j.neuroimage.2011.07.044.
- Vasic, N., Walter, H., Hose, A., & Wolf, R. C. (2008). Gray matter reduction associated with psychopathology and cognitive dysfunction in unipolar depression: A voxel-based morphometry study. *Journal of Affective Disorders*, *109*(1–2), 107–116. doi: 10.1016/j.jad.2007.11.011.
- Weiner, K. S., & Grill-Spector, K. (2010). Sparsely-distributed organization of face and limb activations in human ventral temporal cortex. *Neuroimage*, *52*(4), 1559–1573. doi: 10.1016/j.neuroimage.2010.04.262.
- Willner, P., Scheel-Kruger, J., & Belzung, C. (2013). The neurobiology of depression and antidepressant action. *Neuroscience and Biobehavioral Reviews*, *37*(10 Pt 1), 2331–2371. doi: 10.1016/j.neubiorev.2012.12.007.
- World Health Organization (2008). *The Global Burden of Disease: 2004 Update*. 2004 Update. Geneva, Switzerland: World Health Organization, p. 146.
- Wray, N. R., Ripke, S., Mattheisen, M., Trzaskowski, M., Byrne, E. M., & Abdellaoui, A., ... Major Depressive Disorder Working Group of the Psychiatric Genomics, C. (2018). Genome-wide association analyses identify 44 risk variants and refine the genetic architecture of major depression. *Nature Genetics*, *50*(5), 668–681. doi: 10.1038/s41588-018-0090-3.
- Xia, M., Si, T., Sun, X., Ma, Q., Liu, B., Wang, L., ... Group, D. I.-M. D. D. W. (2019). Reproducibility of functional brain alterations in major depressive disorder: Evidence from a multisite resting-state functional MRI study with 1434 individuals. *Neuroimage*, *189*, 700–714. doi: 10.1016/j.neuroimage.2019.01.074.
- Xu, J., Li, Q., Qin, W., Jun Li, M., Zhuo, C., Liu, H., ... Yu, C. (2018). Neurobiological substrates underlying the effect of genomic risk for depression on the conversion of amnesic mild cognitive impairment. *Brain: A Journal of Neurology*, *141*(12), 3457–3471. doi: 10.1093/brain/awy277.
- Yan, C. G., Wang, X. D., Zuo, X. N., & Zang, Y. F. (2016). DPABI: Data processing & analysis for (resting-state) brain imaging. *Neuroinformatics*, *14*(3), 339–351. doi: 10.1007/s12021-016-9299-4.
- Zang, Y., Jiang, T., Lu, Y., He, Y., & Tian, L. (2004). Regional homogeneity approach to fMRI data analysis. *Neuroimage*, *22*(1), 394–400. doi: 10.1016/j.neuroimage.2003.12.030.
- Zhang, B., & Horvath, S. (2005). A general framework for weighted gene co-expression network analysis. *Statistical Applications in Genetics and Molecular Biology*, *4*, Article17. doi: 10.2202/1544-6115.1128
- Zhang, Y., Sloan, S. A., Clarke, L. E., Caneda, C., Plaza, C. A., Blumenthal, P. D., ... Barres, B. A. (2016). Purification and characterization of progenitor and mature human astrocytes reveals transcriptional and functional differences with mouse. *Neuron*, *89*(1), 37–53. doi: 10.1016/j.neuron.2015.11.013.